Microbial Cell Factories

RESEARCH

Open Access

Development of a lysine biosensor for the dynamic regulation of cadaverine biosynthesis in *E. coli*

Mingjie Li[1,2], Haorong Chen[1,2], Yukun Chen[1,2], Pengyu Chen[1,2], Shuchun Liu[1], Shuwen Liu[1,3*] and Tingyi Wen[1,4*]

Abstract

Background As one of the most promising monomers of biobased polyamides, cadaverine has wide industrial application prospects. However, in microbial cadaverine fermentation with glucose as the sole carbon source, the impaired coordination between precursor (lysine) utilization and cytotoxic cadaverine accumulation has been identified as the primary bottleneck limiting high-yield biosynthesis. Here, we developed a lysine biosensor in *Escherichia coli* to dynamically regulate cadaverine biosynthesis.

Results In this study, we developed a lysine biosensor based on the lysine transporter protein LysP, the transcription activator CadC, and the GFPuv gene under the control of the P_{cad} promoter. However, the engineered lysine biosensor system had a low dynamic range and a narrow pH operating range. Therefore, a multilevel optimization strategy, which included the introduction of key point mutations and engineered promoter modifications, were introduced to improve the performance of the biosensor, resulting in significant improvements in the dynamic range and lysine response. Moreover, we engineered a cadaverine-producing *E. coli* strain by increasing the supply of the lysine precursor, overexpressing key cadaverine synthesis genes, and knocking out genes related to metabolic bypass. The lysine biosensor was subsequently implemented to dynamically regulate cadaverine biosynthesis, resulting in a 48.10% increase in the production titre (33.19 g/L) and a 21.2% increase in cell growth compared with those resulting from the strain with constitutive expression.

Conclusion This is the first report in which a lysine biosensor constructed in *E. coli* could dynamically regulate cadaverine synthesis to improve its yield and biomass. This strategy provides new insights into the metabolic engineering of lysine and its derivatives in *E. coli*.

Keywords Lysine, Cadaverine, Biosensor, Dynamic regulation, *Escherichia coli*

*Correspondence:
Shuwen Liu
liusw@im.ac.cn
Tingyi Wen
wenty@im.ac.cn
[1] State Key Laboratory of Microbial Diversity and Innovative Utilization, Institute of Microbiology, Chinese Academy of Sciences, Beijing 100101, China
[2] University of Chinese Academy of Sciences, Beijing 100049, China
[3] Beijing Key Laboratory of Genetic Element Biosourcing & Intelligent Design for Biomanufacturing, Beijing 100101, China
[4] Medical School, University of Chinese Academy of Sciences, Beijing 100049, China

Background

The central challenge in metabolic engineering is optimizing target product synthesis while preserving cellular viability. Conventional static approaches, which rely on the constitutive overexpression or deletion of genes, often perturb metabolic homeostasis [1, 2]. The accumulation of nonessential or even toxic metabolites during the early stages of fermentation disrupts bacterial porin function, impairing nutrient uptake and triggering growth arrest [3–6]. These limitations highlight the need

for dynamic metabolic flux control strategies that balance biosynthesis with cell proliferation.

Biosensors have emerged as powerful tools for implementing such dynamic regulation [7]. By integrating metabolite-responsive transcriptional or translational control elements into engineered strains, these systems enable the real-time adjustment of metabolic pathways on the basis of intracellular metabolite concentrations [8, 9]. This adaptive approach maintains metabolic network integrity while maximizing product yield.

The lysine derivative cadaverine (1,5-diaminopentane) serves as a critical monomer for biobased polyamide production, yet its cytotoxicity is a significant bottleneck [10, 11]. To improve the tolerance of *Escherichia coli* to cadaverine, Wang et al. [12] engineered bacteria via UV and ARTP mutagenesis to yield a cadaverine-tolerant strain with a 31% increase in production. To mitigate the toxic effects of cadaverine in fermentative production, Gao et al. [13] introduced a thermal switch system to divide the fermentation process into two stages, lysine accumulation and cadaverine synthesis, effectively avoiding the inhibitory effect caused by cadaverine accumulation. However, these methods lack the precision of biosensor-mediated dynamic regulation, which can coordinate cadaverine biosynthesis with cellular growth requirements. Therefore, dynamic regulation strategies that increase the compatibility between bacterial growth and cadaverine production while reducing the inhibitory effects of cadaverine on early bacterial growth are promising strategies for increasing cadaverine production.

In order to achieve dynamic regulation of cadaverine synthesis, we first constructed a lysine biosensor based on the Cad system in *E. coli* in this study. The Cad system in *E. coli*, which responds to acidic stress, consists of the lysine decarboxylase CadA, cadaverine-lysine transporter CadB, and transcription activator CadC. CadC is an integral membrane protein that belongs to the ToxR-like family of transcriptional activators and associates with the lysine transporter LysP within the membrane [14, 15]. When *E. coli* grows in an acidic environment (pH < 5.8), CadC dissociates from LysP and binds to the P_{cad} promoter, thereby inducing the expression of the *cadBA* operon, which decarboxylates lysine to form cadaverine and exports it out of the cell, helping neutralize the external pH and supports bacterial survival under these unfavourable conditions. The functional core of this biosensor includes the lysine transporter LysP, the transcription factor CadC, the promoter P_{cad} of the *cadBA* operon, and its controlled expression of GFPuv.

The lysine biosensor was subsequently improved through a multistage strategy to increase its pH limit and expand its detection range.The starting strain MG1655 was metabolically engineered for cadaverine production, which included gradually increasing the targeted flux of lysine, expressing key genes for cadaverine synthesis, and knocking out the genes involved in cadaverine metabolic bypass. To verify the dynamic regulation of cadaverine synthesis by the constructed lysine sensor, we conducted fermentation tank experiments using the engineered cadaverine-producing bacteria. Finally, compared with traditional static strategies, dynamic regulation with the lysine biosensor can significantly increase the production of cadaverine. This finding indicates that under the control of the biosensor, the dynamically regulated expression of cadaverine synthesis genes is superior to their constitutive expression, balancing the bacterial growth with cadaverine synthesis to significantly improve production. This study provides an example of the dynamic regulation of the synthesis of cadaverine and other lysine derivatives.

Materials and methods

Strains, plasmids, and reagents

All bacterial strains used in this study are listed in Table S1. *E. coli* EC135 [16] was used as a cloning host for plasmid construction, and *E. coli* MG1655 was used for metabolic engineering. Q5 Hot Start high-fidelity DNA polymerase (New England BioLabs) was used to amplify the donor DNA fragments. A DNA Purification Kit, Bacteria DNA Kit and Mini Plasmid Kit from TIANGEN BIOTECH were used for DNA preparation. A Q5 Site-Directed Mutagenesis Kit (New England BioLabs) was used to construct pTargetF plasmids. In addition, 2 × M5 Super FastTaq PCR Master Mix from Mei5Bio (Beijing) was used for colony PCR identification. All primers were synthesized by Tianyi Huiyuan (Beijing). All primers used in this study are listed in Table S2. Tryptone and yeast extracts were obtained from OXOID. Amino acids and antibiotics were purchased from Sigma Aldrich. Unless otherwise specified, all other chemicals were purchased from Beijing Chemical Plant.

Culture medium and conditions

During strain construction, the strains were grown in LB medium at 30 °C or 37 °C. LB medium contained 10 g/L tryptone, 10 g/L NaCl and 5 g/L yeast extract. agar powder of 20 g/L was added to the medium to prepare a solid medium. If needed, kanamycin (50 mg/ml) or spectinomycin (50 mg/ml) can be added to achieve selective culture. During gene deletion and integration, L- (+)—arabinose (final concentration of 10 mM) was used to induce the effects of the CRISPR/Cas9 system and the red homologous recombination system.

To analyse the expression of green fluorescent protein in shake flask fermentation, a ring of cells was inoculated into a 50 ml tube with 5 ml of LB medium,

incubated at 37 °C for 8 h, and shaken at 220 rpm on a rotary shaker. Then, 1% (v/v) seed culture was inoculated into a 500 ml flask containing 25 ml shaking flask fermentation MOPS medium containing 20 g/L glucose, 8 g/L $(NH_4)_2SO_4$, 2 g/L KH_2PO_4, 2 g/L $MgSO_4{\cdot}7H_2O$, 5 g/L yeast extract, 80 g/L MOPS, and 2 ml/L trace element mixture, and the pH was adjusted to 7.6, 7.0 or 5.8 with ammonia or hydrochloric acid. Lysine hydrochloride at different concentrations was subsequently added to the shake flask after 12 h of fermentation to induce the expression of fluorescent proteins.

For fed-batch fermentation of the 5 L bioreactor, one loop of cells was inoculated into a 50 mL tube with 5 mL of LB medium and incubated for 12 h at 37 °C with shaking at 220 rpm on a rotary shaker for preculture. For the seed culture, 500 µL of the obtained preculture broth was inoculated into 50 mL of seed culture under the same culture conditions for 6 h. Then, 100 mL of seed medium was inoculated into a 5 L bioreactor with a final volume of 2 L. The formulation of the fed-batch fermentation medium was as follows: 10.0 g/L glucose, 5.0 g/L yeast powder, 15.0 g/L $(NH_4)_2SO_4$, 2.0 g/L betaine, 1.6 g/L KH_2PO_4, 1.5 g/L $MgSO_4$, 0.03 g/L $FeSO_4$, 0.03 g/L $MnSO_4$, 0.08 g/L pyridoxal phosphate, and 4 mL trace element mixture. The pH was maintained at 6.8–7.0 by adding ammonia water. The dissolved oxygen (DO) level was maintained at approximately 30%, and the stirring speed was 350–800 rpm. When the initial glucose concentration was less than 5 g/L, additional feed glucose (the original solution contained 625 g/L glucose, $MgSO_4.7H_2O$ 5 g/L, and $(NH_4)_2SO_4$ 100 g/L) was added to maintain the residual sugar concentration at 10 g/L.

The trace element solutions were prepared as follows [17]: $FeSO_4{\cdot}7H_2O$ 6 g/L, $CaCl_2$ 1.35 g/L, $ZnSO_4{\cdot}7H_2O$ 0.8 g/L, $MnSO_4{\cdot}4H_2O$ 1.5 g/L, $CuSO_4{\cdot}5H_2O$ 0.15 g/L, $(NH_4)_6Mo_7O_{24}{\cdot}4H_2O$ 0.2 g/L, H_3BO_3 0.1 g/L, $CoCl_2{\cdot}6H_2O$ 0.25 g/L, and 35% HCl 10 mL.

Construction of strains and plasmids

A Q5 site-specific mutagenesis kit was used to construct pTargetF plasmids with different N20 sgRNA sequences. All the donor DNA templates were obtained through overlapping PCR via 2×Phanta Flash Master Mix DNA Polymerase. As previously reported [18], all *E. coli* gene knockouts were performed through the CRISPR/Cas9 genome editing process. All plasmids were constructed via seamless cloning kits from Beijing Jinsha Biological Company. All transformants were identified through colony PCR, and DNA sequencing was performed at Tianyi Huiyuan (Beijing).

Analysis methods

The optical density (OD_{600}) was measured at 600 nm via a UV spectrophotometer to monitor the biomass concentration. The dry cell weight (DCW) was calculated on the basis of the OD_{600} (1 OD_{600} = 0.42 g DCW/L) [19].

The fermentation broth was centrifuged at 8000×g for 5 min, and the supernatant was collected for substrate and product concentration analysis. The glucose concentration was measured via an enzyme electrode analyzer containing glucose oxidase (SBA-40D; Shandong Institute of Biology, China) [17].

The concentration of the product in the fermentation culture supernatant was determined via HPLC as previously described [20]. An AdvanceBio AAA column (4.6 mm×150 mm, 5 mm; Agilent Technology, USA) was used at 40 °C after automated online derivatization using O-phthalaldehyde (OPA). Elution was performed via a gradient of reagent A (10 mM Na_2HPO_4 and 10 mM $Na_2B_4O_7$, pH 8.2 by HCl) and reagent B (methanol/acetonitrile/water = 45:45:10, by vol.) at 1 mL/min. The elution gradient was as follows: 0–0.35 min, 2% B; 13.4 min, 57% B; 13.5 min, 100% B; 15.7 min, 100% B; 15.8 min, 2% B; and 18 min, 2% B. The eluate was monitored at 338 nm.

A multifunctional microplate reader (TECAN multifunctional microplate reader spark, Switzerland) was used to measure the luminescence value of the green fluorescent protein. The fermentation broth to be detected was added to a Corning 96 flat black plate at 200 µl per well in triplicate. The excitation wavelength of GFP was set at 395 nm, the excitation bandwidth was 20 nm, the emission wavelength was set at 509 nm, and the emission bandwidth was 20 nm. The other parameters used were as follows: gain manual: 60%, 50% mirror integration time: 40 µs. The OD value of the fermentation broth was measured at a wavelength of 600 nm. The relative GFP value is the GFP value divided by the OD_{600}.

The method for determining lysine decarboxylase activity and the definition of enzyme activity were based on previous study [21]. For lysine decarboxylase (CadA) activity assay, cells were harvested by centrifugation at 8,000×g for 5 min and washed twice with a cold buffer containing 100 mM Tris–HCl (pH 7.5), 100 mM KCl, 5 mM $MgCl_2$, and then resuspended in the same buffer supplying 1 mM DTT. Cells were sonicated on ice for 10 min (a working period of 3 s in a 3-s interval for each cycle) at a power output of 200 W by an ultrasonic disruptor (XC-IID, Xinchen, Beijing, China). The cell debris were removed by centrifugation (12,000×g for 60 min at 4 °C), and the resulting crude cell extracts were immediately used for determination of specific enzyme activities. The total protein concentration in crude cell extract was measured

by Bradford's method with bovine serum albumin as a standard. Then, 20 mM of lysine-HCl and 0.1 mM pyridoxal phosphate were added to the sodium acetate buffer (pH 6), incubated at 37 °C and 220 rpm in a rotary oscillator for 30 min, and heated at 100 °C for three minutes to stop the reaction. The concentration of cadaverine was then detected. The enzyme activity was defined as follows: 1 U/mg was defined as 1 μmol of cadaverine was produced by 1 mg crude cell extracts per minute, which is modified from other's definition [22].

Results and discussion

Construction and validation of the lysine biosensor

In acidic environments and in the presence of lysine, CadC dissociates from LysP and binds to the P_{cad} promoter, thereby inducing the expression of the *cadBA* operon [23] (Fig. 1A). To design a biosensor that responds to changes in the extracellular lysine concentration, we constructed a genetic module incorporating the lysine transporter LysP and the transcriptional regulator CadC from *E. coli* (Sensor-2). In the control group (Sensor-1), only the transcriptional regulator CadC was included. The P_{cad} promoter of the *cadBA* operon, along with its

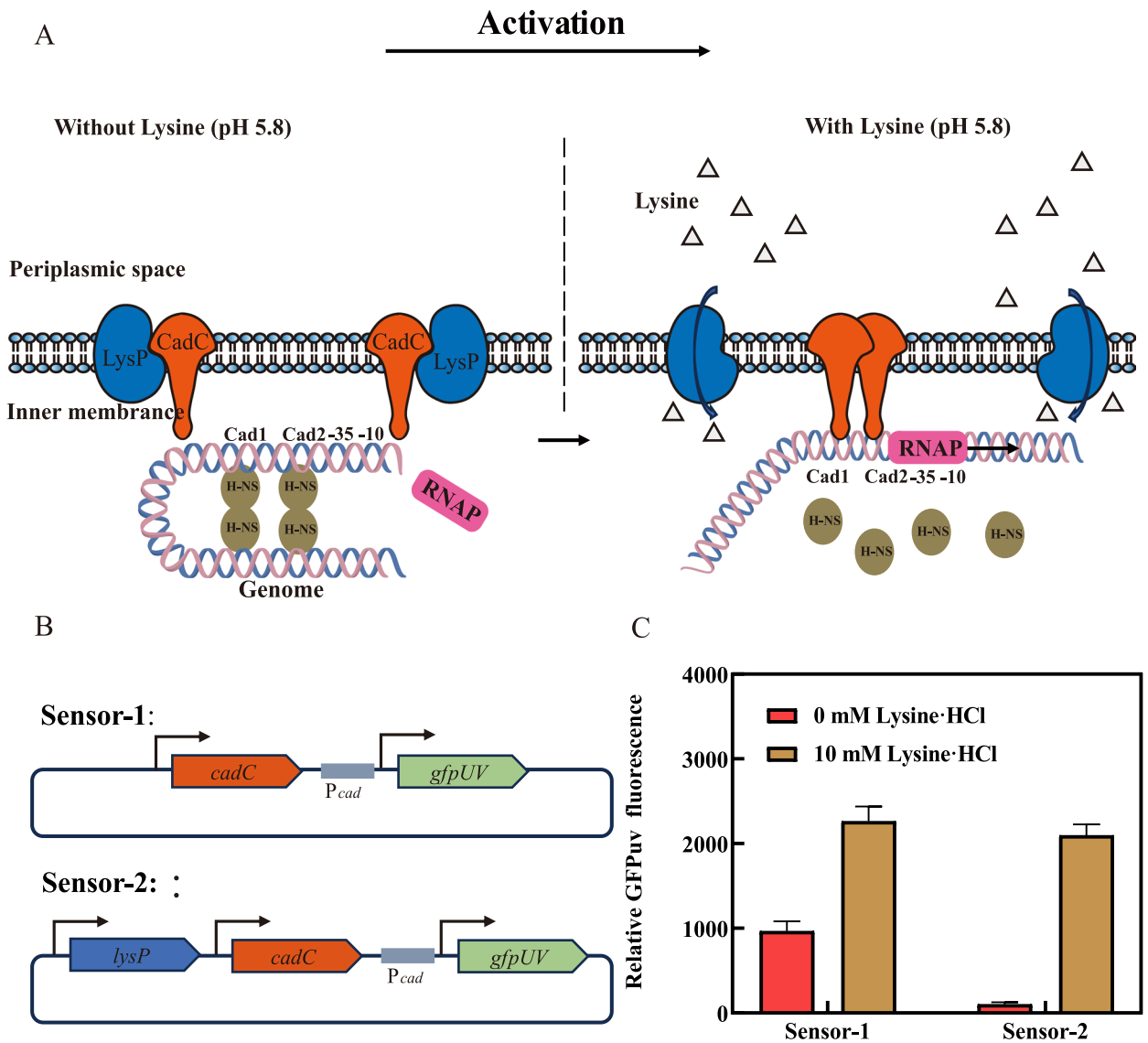

Fig. 1 Schematic and verification of the designed lysine biosensor. **A** Diagram demonstrating the principle of the lysine biosensor. **B** Basic components of the lysine biosensor. **C** Relative green fluorescence intensities of Sensor-1 and Sensor-2 in the presence and absence of 10 mM lysine. The error bars represent the standard deviation from three independent measurements

upstream regulatory sequence, was cloned upstream of the GFPuv gene, setting GFPuv expression under the control of P_{cad} (Fig. 1B).

To evaluate the functionality of the lysine biosensor, the constructed plasmid was introduced into the wild-type *E. coli* strain MG1655 for overnight cultivation in shake flasks with or without lysine hydrochloride supplementation. Afterwards, the cultures were transferred to 96-well plates, and the fluorescence intensity was measured using a multifunctional microplate reader. The results revealed that cells containing Sensor- 1 and Sensor-2 exhibited significant differences in fluorescence intensity (Fig. 1C). In the absence of added lysine, Sensor-1 exhibited high baseline fluorescence, suggesting that the intracellular expression of CadC exceeded that of LysP, resulting in constitutive expression of GFPuv. Notably, Sensor-2 could reliably indicate the presence or absence of extracellular lysine.

Construction and characterization of a pH-independent lysine sensor

During the fermentation process of *E. coli*, the optimal pH for *E. coli* fermentation is approximately neutral (pH 6.8–7.0), and activating the sensor under acidic conditions (pH < 5.8) would limit its application. A cluster of negatively charged amino acids (Asp-198, Asp-200, Glu-461, Glu-468, and Asp-471) in CadC was found to be crucial for pH sensing [24]. These residues form a negatively charged region on the surface of the CadC periplasmic domain, which also affects the dimerization of CadC under alkaline conditions. Protonation of this negatively charged domain reduces electrostatic repulsion between two CadC monomers, affecting dimerization [25]. Among these point mutations, only the point mutation $CadC^{D471N}$ is the most stable in inducing *cadBA* under acidic or alkaline conditions [24]. To eliminate the pH dependency of Sensor-2, we mutated the amino acid 471 of CadC from aspartate to the basic amino acid asparagine [24], resulting in the construction of Sensor-3 (Fig. 2A). The performance of Sensor-2 and Sensor-3 was evaluated in acidic and alkaline environments. To evaluate the impact of $CadC^{D471N}$ introduction, validation of the sensor was conducted under both mildly acidic (pH 5.8) and alkaline (pH 7.6) conditions. The results showed that, owing to the introduction of this point mutation, Sensor-3 did not exhibit the pH limitation of Sensor-2

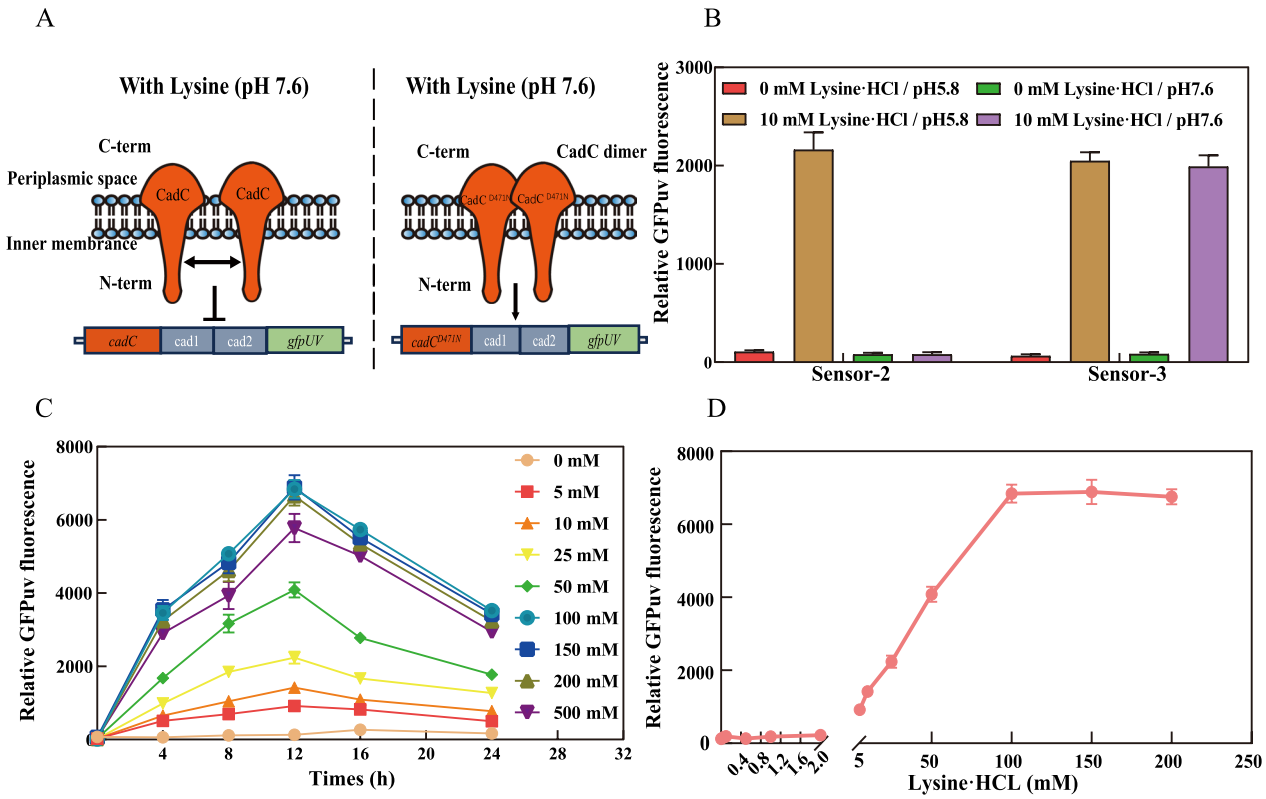

Fig. 2 Construction and characterization of a pH-independent lysine sensor. **A** Schematic of the $CadC^{D471N}$ mutant that removes the pH limitation of the sensor. **B** Relative green fluorescence intensities of Sensor-2 and Sensor-3 with and without 10 mM lysine hydrochloride supplementation at pH 5.8 or pH 7.6. **C** Relative green fluorescence intensities of Sensor-3 after different induction durations and supplementation with various concentrations of lysine hydrochloride. **D** Characterization of the pH-independent Sensor-3

and could be activated by lysine under both acidic and alkaline conditions (Fig. 2B).

Additionally, the relative fluorescence intensity was determined after different induction durations. The results revealed that the relative green fluorescence intensity of the lysine biosensor peaked after 12 h of induction. Consequently, the fluorescence intensity at the 12-h mark was used in subsequent experiments to characterize the sensor. Further characterization of Sensor-3 revealed that GFPuv expression was negligible at lysine concentrations less than 5 mM (Fig. S1), but the biosensor exhibited a good linear response within the lysine concentration range of 5–100 mM (Fig. 2C, D). Thus, Sensor-3 effectively and accurately reflects the dynamic changes in the extracellular lysine content.

When the concentration of lysine exceeded 200 mM, the expression of GFPuv decreased. High-performance liquid chromatography (HPLC) analysis of the fermentation broth revealed that the exogenously added lysine was converted to cadaverine (Fig. S2). Once the extracellular concentration of cadaverine surpasses a certain threshold, it exerts results in negative feedback on the transcriptional activator CadC. Cadaverine then binds to the central cavity of CadC, presumably triggering an intramolecular rearrangement that exposes the cadaverine binding site at the dimer interface, thereby inactivating CadC and subsequently shutting down the transcription of the *cadBA* operon [26]. The inhibition of CadC activity resulted in a decrease in GFPuv, affecting the performance of the sensor.

Multilevel strategy to improve lysine sensor performance

In previous studies, partial mutants of *cadC* enhanced feedback inhibition of cadaverine. The $CadC^{Y453I}$ mutant exhibited reduced inhibition, likely due to the weak affinity of the mutant for cadaverine at the dimer interface [26]. To counteract *cadC* inhibition by cadaverine, we introduced a point mutation to generate the mutant $CadC^{Y453I}$ and construct Sensor-4 (Fig. 3A). Deleting the cad operon from the *E. coli* genome can prevent biosensor activation by wild-type CadC and ensure that only the plasmid controls GFP expression. Incorporating this deletion into Sensor-4 led to the construction of Sensor-5 (Fig. 3A).

Introduction of the $CadC^{Y453I}$ mutant into the sensor weakened the cadaverine-mediated feedback inhibition of the biosensor, which increased the dynamic range of Sensor-4 by 58% compared with that of Sensor-3. In addition, compared with Sensor-3, further knockout of the cad system in the MG1655 chromosome in Sensor-5 increased the dynamic range by approximately 153% and exhibited an expanded lysine detection range of 5–150 mM (Fig. 3B).

Engineering the promoters of the key components of a sensor is a conventional strategy to increase the sensitivity and detection range of biosensors to meet specific requirements [27]. Previous experiments in Sensor-1 have demonstrated that excessive CadC leads to constitutive expression of GFPuv. The constructed lysine biosensor combines LysP and CadC to sense external lysine, and the ratio of the expression levels of the membrane proteins LysP and CadC affects the detection range of the lysine biosensor. The expression of green fluorescent protein was only observed in Sensor-2 which contained the natural promoter LysP and CadC when lysine was added, indicating that the expression of LysP in the natural promoter was higher than that in CadC. Moreover, the overexpression of *E. coli* membrane proteins may cause cytotoxicity and severely impair cell growth. Therefore, we employed the Anderson promoters P_{J23109} and P_{J23114}, which have medium and low intensities, respectively, to regulate the expression of LysP and CadC (Fig. 3C).

The current biosensor pSenlys, which is based on LysG, a transcription regulator of *Corynebacterium glutamicum*, has been successfully applied in the screening of lysine-producing bacteria [28, 29]. In *C. glutamicum*, LysG, as a transcriptional activator of LysE, can sense how the intracellular lysine concentration changes in response to different arginine or histidine concentrations [30]. On this basis, Liu et al. [31] screened the lysine-sensitive mutant LysG and improved the specificity of the biosensor. However, these series of biosensors are all based on *C. glutamicum*, and their application in *E. coli* does not yield satisfactory results [32]. Moreover, the lysine riboswitch of the aspartate kinase III gene (*lysC*) in *E. coli* was used to construct a lysine biosensor that was used for developing high-throughput screening (HTS) methods to optimize phosphoenolpyruvate carboxylase expression or screen for bacteria that produce lysine in high yield [33, 34]. However, the maximum detection range of the sensor based on the *lysC* ribosome switch is only 10 g/L (approximately 68 mM), which also limits its application. Therefore, it is necessary to develop a lysine biosensor suitable for *E. coli*. By modifying the promoter of the biosensors, the lysine detection range of Sensor-7 was further improved to 200 mM (Fig. 3D). Additionally, 200 mM is currently the highest response threshold of lysine biosensors in *E. coli*, and dynamic control will subsequently be tested on Sensor-7. The current selection of CadC mutants primarily relies on known sites reported in the literature, while a systematic exploration of all potential functional sites has yet to be conducted. In the future, directed evolution or rational design could be employed to identify better-optimized key components for the sensor.

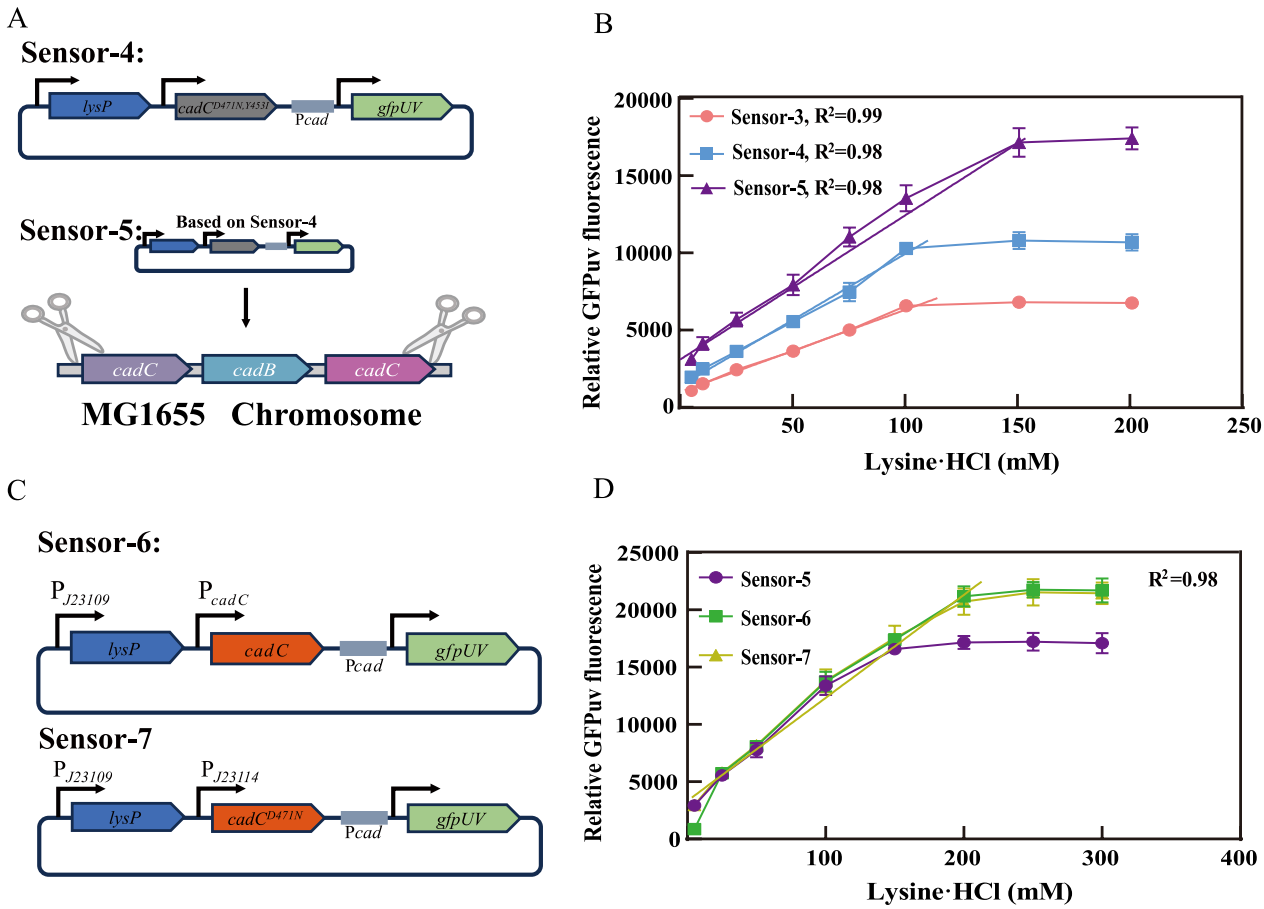

Fig. 3 Multilevel strategy to improve the performance of lysine biosensors. **A** Schematics of how the inhibitory effect of cadaverine on CadC is reduced with Sensor-4 and Sensor-5. **B** Characterization of the dynamic response ranges of Sensor-4 and Sensor-5 to lysine hydrochloride. **C** Engineered modifications in the promoters of Sensor-6 and Sensor-7. **D** Characterization of the dynamic response ranges of Sensor-6 and Sensor-7 to lysine hydrochloride

Metabolic engineering of cadaverine-producing bacteria

In the metabolic engineering of the cadaverine-producing strain depicted in Fig. 4A, glucose serves as the carbon source for cadaverine biosynthesis in *E. coli*. The key precursor phosphoenolpyruvate (PEP) is carboxylated to oxaloacetate by phosphoenolpyruvate carboxylase (encoded by *ppc*). Oxaloacetate is subsequently transaminated to aspartate, which then undergoes phosphorylation by aspartate kinase (encoded by *lysC*) to yield β-aspartyl phosphate in an ATP-dependent reaction. This enzyme represents the primary rate-limiting step of the pathway and is subject to strong feedback inhibition by the end-product lysine, ensuring precise flux control.

β-Aspartyl phosphate is then reduced to aspartate semialdehyde by aspartate semialdehyde dehydrogenase (encoded by *asd*). Aspartate semialdehyde is sequentially converted through the diaminopimelate (DAP) pathway via multiple enzymatic steps to yield the direct biosynthetic precursor of lysine (meso-DAP). Dihydrodipyridine carboxylic acid synthase (encoded by *dapA*) inhibited by its end-product lysine, is the key regulatory enzyme in the DAP pathway. Afterwards, diaminopimelate decarboxylase (encoded by *lysA*), which governs the final step of lysine biosynthesis, catalyzes the decarboxylation of DAP to lysine, releasing CO_2. There are two lysine decarboxylases: CadA and LdcC. CadA is preferentially utilized for cadaverine production due to its superior substrate affinity. Finally, cadaverine is exported extracellularly by the energy-dependent cadaverine-lysine antiporter CadB.

To construct cadaverine-producing bacteria, *cadBA* was expressed under the control of the P_{trc} promoter in the plasmid pBR322. This plasmid was subsequently transformed into MG1655 Δ*cadCBA* to obtain the strain PDA. The subsequent focus was on increasing the supply of lysine precursors. In order to increase the flux of carbon towards lysine, the genes encoding feedback-resistant $lysC^{T344M}$ [35] and *lysA* were simultaneously

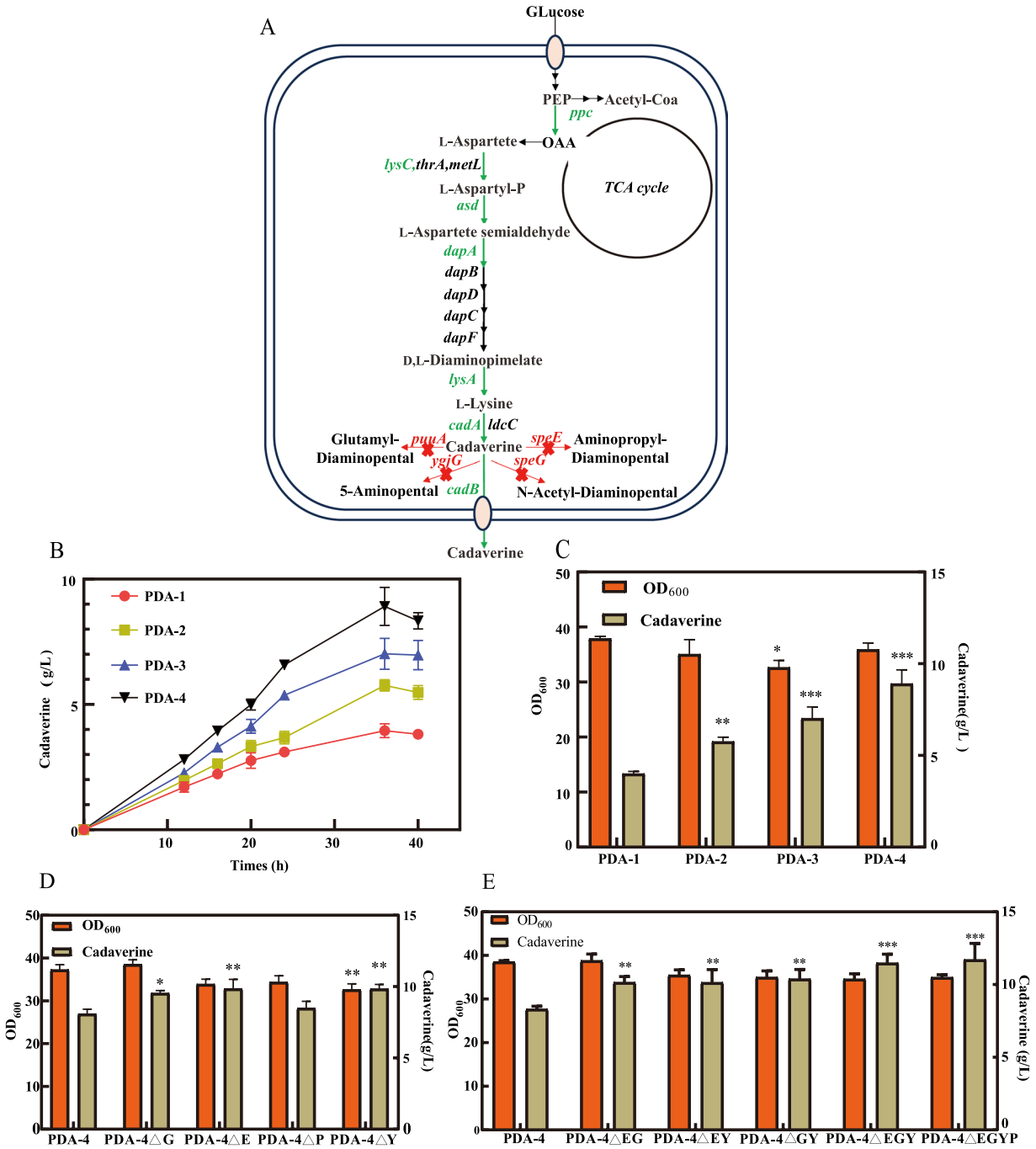

Fig. 4 Metabolic engineering and fermentation validation of cadaverine producing strains. **A** Metabolic engineering modifications of cadaverine-producing strains. The genes with green arrows indicate overexpression, and the genes with red arrows represent knockouts. **B** Curves of cadaverine production by PDA-1, PDA-2, PDA-3, and PDA-4 during shake flask fermentation. **C** The OD_{600} values and cadaverine yields of PDA-1, PDA-2, PDA-3, and PDA-4 during shake flask fermentation. **D**, **E** Effects of the knockout of various cadaverine metabolic bypass genes on the yield of cadaverine

cloned and inserted into the plasmid pACYC184, which was subsequently transformed into PDA to obtain PDA-1. Moreover, the genes *asd* and feedback-resistant mutant $dapA^{H56K}$ [35] were also overexpressed to obtain the PDA-2 strain, further increasing carbon flux into the lysine synthesis pathway. To enhance the metabolic flux from PEP towards lysine biosynthesis, the key gene *ppc* was also overexpressed to obtain the strain PDA-3. In

order to verify the dynamic regulation of cadaverine by the sensor, the component *gfpuv* of sensor-7 was replaced with *cadBA*, and the modified plasmid was introduced into the strain MG1655Δ*cadCBA* along with the lysine production plasmid, thus producing the strain PDA-4.

Then, the effects of these strains on cadaverine production were compared through shake flask fermentation experiments. As shown in Fig. 4B, C, the cadaverine production of PDA-3 reached 7.9 g/L after 36 h, representing a 79% increase compared with that of PDA-1. This finding indicates that as the expression of key lysine synthesis genes gradually increased, the yield of cadaverine significantly increased. Furthermore, when the lysine sensor was used to dynamically regulate cadaverine synthesis, the cadaverine yield of PDA-4 was 25.6% higher than that of PDA-3, which was expressed under the constitutive promoter P_{trc}. These shake flask results demonstrate that our lysine biosensor can significantly improve cadaverine production.

Native cadaverine production is related to lysine decarboxylation by CadA. However, cadaverine is further utilized through the actions of 4 genes to produce byproducts, decreasing cadaverine accumulation, as shown in Fig. 4A. These genes include *speE*, which encodes a cadaverine/cadaverine aminopropyltransferase; *puuA*, which encodes a glutamate-cadaverine/glutamate cadaverine ligase; *speG*, which encodes spermidine acetyltransferase; and *ygjG*, which encodes another cadaverine/cadaverine aminotransferase [36–38]. To minimize the degradation of cadaverine and further increase its production, we individually knocked out four genes. The genetic deletion mutants are abbreviated as follows: ΔG (Δ*speG*), ΔE (Δ*speE*), ΔP (Δ*puuA*) and ΔY (Δ*ygjG*). Subsequently, the resulting strains, PDA-4ΔG, PDA-4ΔE, PDA-4ΔP and PDA-4ΔY, were verified through shake flask fermentation. As shown in Fig. 4D, knockout of puuA had little effect on the production of cadaverine. However, compared with those of the unmodified PDA-4 strain, individual deletion of *speE*, *puuA*, and *speG* led to significant increases in the production of cadaverine by 18.1%, 22.1%, and 25.2%, respectively.

The genes *speE*, *speG*, and *ygjG*, which primarily influence cadaverine synthesis, were subsequently deleted in various combinations to obtain five strains: PDA-4ΔEG, PDA-4ΔEY, PDA-4ΔGY, PDA-4ΔEGY and PDA-4ΔEGYP. The effects of these combined gene deletions on cadaverine production were compared through shake flask fermentation. Compared with that of the unmodified strain PDA-4, the cadaverine production of PDA-4ΔEGYP, whose metabolic pathway was completely blocked, increased by 37%, reaching 11.69 g/L (Fig. 4E). These findings demonstrate that inhibiting the degradation of cadaverine plays a crucial role in enhancing its production.

Dynamic regulation of cadaverine biosynthesis with a lysine biosensor in a 5 L fermenter

In dynamic metabolic engineering and synthetic biology systems, biosensors respond to specific metabolites, modulating the expression of target genes to fine-tune metabolic fluxes and optimize product yield [39]. To inhibit the early growth of bacterial cells via cadaverine, we attempted to dynamically regulate cadaverine synthesis via the constructed lysine biosensor Sensor-7. The dynamic regulation principle of the biosensor constructed in this study for cadaverine synthesis is as follows (Fig. 5A). During the early growth phase, lysine gradually accumulates in the broth. When the extracellular lysine concentration reaches a certain threshold, a portion of the lysine reenters the cell, triggering the expression of cadaverine synthesis genes. By dynamically adjusting the synthesis of cadaverine, the compatibility between the synthesis of precursor lysine and cadaverine production can be enhanced. The intracellular lysine is promptly converted into cadaverine and transported out of the cell without lysine accumulation or feedback inhibition. Compared with adding exogenous inducers such as IPTG, using lysine naturally produced by bacterial cells as an inducer to dynamically regulate the synthesis of cadaverine has lower costs, less cell damage, and simpler downstream purification processes. The previous shake flask fermentation results demonstrated that our sensor effectively dynamically regulates the synthesis of cadaverine. The copy number of plasmids can affect cell growth rate, gene expression, biosynthesis, and genetic circuit performance. Each plasmid imposes a linear metabolic burden of 0.063% on its host, suggesting a simple relationship between metabolic burden and plasmid DNA synthesis [40]. In the present study, we developed a single-plasmid system through the integration of both dynamic regulation and lysine production modules into the pBR322 backbone. However, the medium-copy-number nature of this chimeric plasmid appears to have created substantial metabolic load on the host cells, leading to compromised cellular growth and reduced cadaverine production efficiency (Fig.S3). To reduce the metabolic burden on cell growth caused by both plasmids and double resistance, we integrated the sensor plasmid and the cadaverine production plasmid into a single plasmid and replaced the low copy number replicon pSC-101.

Owing to limitations in the supply of nutrients and dissolved oxygen, as well as other factors, the production capacity of a strain may not be fully demonstrated in shake flask cultures. To comprehensively assess the overall cadaverine production by the strain PDA-6 upon

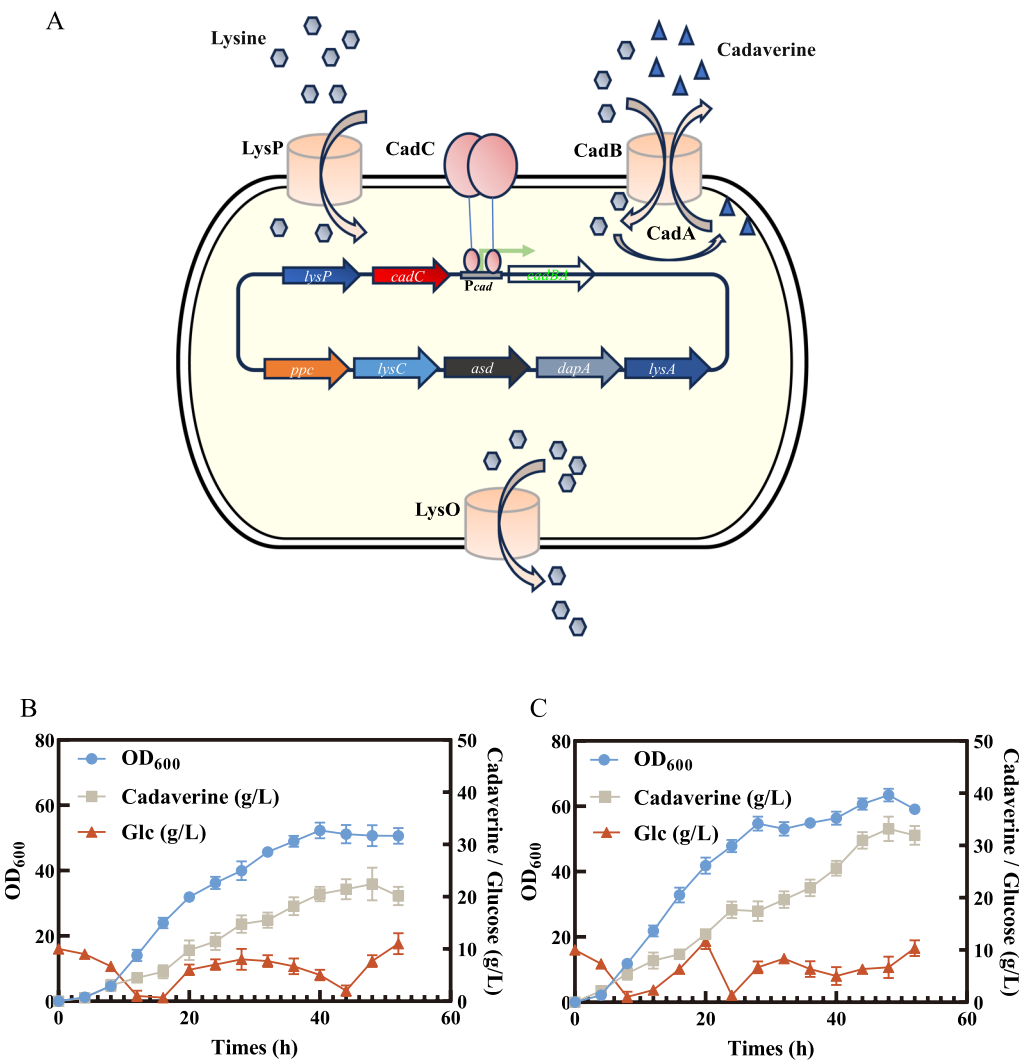

Fig. 5 Schematic diagram of dynamic regulation of cadaverine synthesis and fed-batch fermentation of cadaverine in 5-L fermenter. **A** Schematic of the mechanism by which the lysine biosensor dynamically regulates cadaverine synthesis. **B**, **C** Batch fermentation curves of PDA-5 and PDA-6 strains fed in 5-L fermenter

dynamic regulation by the lysine sensor, fed-batch fermentation was carried out in a 5 L bioreactor, with the PDA-5 strain serving as the control. Compared with PDA-5, which exhibits constitutive expression under the control of P_{trc}, PDA-6 exhibited superior bacterial growth throughout the fermentation period, with increases in biomass of 21.2% and the maximum cadaverine production of approximately 48.10% compared with those of PDA-5 (Fig. 5B, C). Analysis of enzyme activity in strains PAD-5 and PDA-6 harvested at the growth stage. As shown in Fig.S4, CadA activity in strain PDA-6 at this stage was approximately 45% lower than in PAD-5. This indicates that a low level of *cadA* expression is sufficient for cadaverine synthesis from lysine. These results empirically validate that flux balance mediated by biosensors is superior to constitutive expression strategies by addressing the fundamental trade-off between pathway activity and cellular adaptability in industrial scale biological processes.

Conclusions

In this study, a lysine biosensor in *E. coli* was designed. Through multistage modification, a pH-independent lysine biosensor was successfully obtained with a maximum detection range of 200 mM. Moreover, the constructed lysine biosensor can dynamically regulate the synthesis of cadaverine, balance bacterial growth with cadaverine accumulation, and effectively improve cadaverine production. The lysine biosensor developed in this study and its dynamic regulation strategy for cadaverine

synthesis not only provide efficient tools for cadaverine biosynthesis, but may also be extended to metabolic engineering applications of other lysine derivatives.

Abbreviations

CRISPR	Clustered regularly interspaced short palindromic repeat
sgRNA	Single-guide RNA
bp	Base pairs
E. coli	*Escherichia coli*
HPLC	High-performance liquid chromatography
OD_{600}	Optical density at wavelength (λ) 600 nm

Supplementary Information

The online version contains supplementary material available at https://doi.org/10.1186/s12934-025-02772-3.

Supplementary material 1.

Acknowledgements
Not applicable.

Author contributions
W.T.Y, L.S.W, and L.M.J conceived and designed the study. L.M.J, C.H.R, and C.Y.K performed the experiments and all data analysis with assistance from C.Y.K, C.P.Y and L.S.C. L.M.J, L.S.W, and W.T.Y wrote and revised the manuscript. All authors read and approved the final manuscript.

Funding
This work was supported by the National Key R&D Program of China (2021YFC2101800) and grant from Beijing Municipal Science & Technology Project, China (No. Z241100007724009).

Availability of data and materials
No datasets were generated or analysed during the current study.

Declarations

Ethics approval and consent to participate
Not applicable.

Consent for publication
Not applicable.

Competing interests
The authors declare no competing interests.

Received: 31 March 2025 Accepted: 16 June 2025
Published online: 21 June 2025

References

1. Snoeck S, Guidi C, De Mey M. "Metabolic burden" explained: stress symptoms and its related responses induced by (over)expression of (heterologous) proteins in *Escherichia coli*. Microb Cell Fact. 2024;23:96.
2. Zhang Q, Wang X, Luo H, Wang Y, Wang Y, Tu T, Qin X, Su X, Huang H, Yao B, et al. Metabolic engineering of Pichia pastoris for myo-inositol production by dynamic regulation of central metabolism. Microb Cell Fact. 2022;21:112.
3. Kaczmarek JA, Prather KLJ. Effective use of biosensors for high-throughput library screening for metabolite production. J Ind Microbiol Biotech. 2021;48:kuab049.
4. Chen XL, Liu LM. Gene circuits for dynamically regulating metabolism. Trends Biotechnol. 2018;36:751–4.
5. Gong XY, Zhang RH, Wang J, Yan YJ. Engineering of a trpR-based biosensor for altered dynamic range and ligand preference. ACS Synth Biol. 2022;11:2175–83.
6. Zhou SH, Alper HS, Zhou JW, Deng Y. Intracellular biosensor-based dynamic regulation to manipulate gene expression at the spatiotemporal level. Crit Rev Biotechnol. 2023;43:646–63.
7. Hong K-Q, Zhang J, Jin B, Chen T, Wang Z-W. Development and characterization of a glycine biosensor system for fine-tuned metabolic regulation in *Escherichia coli*. Microb Cell Fact. 2022;21:56.
8. Marsafari M, Ma J, Koffas M, Xu P. Genetically-encoded biosensors for analyzing and controlling cellular process in yeast. Curr Opin Biotechnol. 2020;64:175–82.
9. Hossain GS, Saini M, Miyake R, Ling H, Chang MW. Genetic biosensor design for natural product biosynthesis in microorganisms. Trends Biotechnol. 2020;38:797–810.
10. Chae TU, Ahn JH, Ko YS, Kim JW, Lee JA, Lee EH, Lee SY. Metabolic engineering for the production of dicarboxylic acids and diamines. Metab Eng. 2020;58:2–16.
11. Kind S, Wittmann C. Bio-based production of the platform chemical 1,5-diaminopentane. Appl Microbiol Biotechnol. 2011;91:1287–96.
12. Wang X, Guo X, Wang J, Li H, He F, Xu S, Chen KQ, Ouyang PK. Ameliorating end-product inhibition to improve cadaverine production in engineered *Escherichia coli* and its application in the synthesis of bio-based diisocyanates. Synth Syst Biotechnol. 2021;6:243–53.
13. Gao SY, Lu JC, Wang TT, Xu S, Wang X, Chen KQ, Ouyang PK. A novel co-production of cadaverine and succinic acid based on a thermal switch system in recombinant *Escherichia coli*. Microb Cell Fact. 2022;21:248.
14. Auger EA, Redding KE, Plumb T, Childs LC, Meng SY, Bennett GN. Construction of lac fusions to the inducible arginine and lysine decarboxylase genes of *Escherichia coli* K-12. Mol Microbiol. 1989;3:609–20.
15. Soksawatmaekhin W, Kuraishi A, Sakata K, Kashiwagi K, Igarashi K. Excretion and uptake of cadaverine by CadB and its physiological functions in *Escherichia coli*. Mol Microbiol. 2004;51:1401–12.
16. Zhang GQ, Wang WZ, Deng AH, Sun ZP, Zhang Y, Liang Y, Che YS, Wen TY. A mimicking-of-DNA-methylation-patterns pipeline for overcoming the restriction barrier of bacteria. PLos Genet. 2012;8:e1002987.
17. Liu SW, Xiao HH, Zhang FF, Lu Z, Zhang Y, Deng AH, Li ZC, Yang C, Wen TY. A seamless and iterative DNA assembly method named PS-Brick and its assisted metabolic engineering for threonine and 1-propanol production. Biotechnol Biofuels. 2019;12:180.
18. Jiang Y, Chen B, Duan CL, Sun BB, Yang JJ, Yang S. Multigene editing in the *Escherichia coli* genome via the CRISPR-Cas9 system. Appl Environ Microbiol. 2015;81:2506–14.
19. Liu Q, Liang Y, Zhang Y, Shang XL, Liu SW, Wen JF, Wen TY. YjeH is a novel exporter of L-methionine and branched-chain amino acids in *Escherichia coli*. Appl Environ Microbiol. 2015;81:7753–66.
20. Li ZC, Liu Q, Sun JH, Sun JJ, Li MJ, Zhang Y, Deng AH, Liu SW, Wen TY. Multivariate modular metabolic engineering for enhanced L-methionine biosynthesis in *Escherichia coli*. Biotechnol Biofuels. 2023;16:101.
21. Liu SW, Liang Y, Liu Q, Tao TT, Lai SJ, Chen N, Wen TY. Development of a two-stage feeding strategy based on the kind and level of feeding nutrients for improving fed-batch production of l-threonine by *Escherichia coli*. Appl Microbiol Biotechnol. 2013;97:573–83.
22. Rui JQ, You SP, Zheng YX, Wang CY, Gao YT, Zhang W, Qi W, Su RX, He ZM. High-efficiency and low-cost production of cadaverine from a permeabilized-cell bioconversion by a Lysine-induced engineered *Escherichia coli*. Bioresour Technol. 2020;302:122844.
23. Tetsch L, Koller C, Haneburger I, Jung K. The membrane-integrated transcriptional activator CadC of *Escherichia coli* senses lysine indirectly via the interaction with the lysine permease LysP. Mol Microbiol. 2008;67:570–83.
24. Haneburger I, Eichinger A, Skerra A, Jung K. New insights into the signaling mechanism of the pH-responsive, membrane-integrated transcriptional activator CadC of *Escherichia coli*. J Biol Chem. 2011;286:10681–9.
25. Lindner E, White SH. Topology, dimerization, and stability of the single-span membrane protein CadC. J Mol Biol. 2014;426:2942–57.
26. Haneburger I, Fritz G, Jurkschat N, Tetsch L, Eichinger A, Skerra A, Gerland U, Jung K. Deactivation of the E. coli pH stress sensor CadC by cadaverine. J Mol Biol. 2012;424:15–27.
27. Dacquay LC, McMillen DR. Improving the design of an oxidative stress sensing biosensor in yeast. Fems Yeast Res. 2021;21:25.

28. Binder S, Schendzielorz G, Stäbler N, Krumbach K, Hoffmann K, Bott M, Eggeling L. A high-throughput approach to identify genomic variants of bacterial metabolite producers at the single-cell level. Genome Biol. 2012;13:R40.
29. Kortmann M, Mack C, Baumgart M, Bott M. Pyruvate carboxylase variants enabling improved lysine production from glucose identified by biosensor-based high throughput fluorescence-activated cell sorting screening. ACS Synth Biol. 2019;8:274–81.
30. Bellmann A, Vrljic M, Pátek M, Sahm H, Krämer R, Eggeling L. Expression control and specificity of the basic amino acid exporter LysE of *Corynebacterium glutamicum*. Microbiol-Sgm. 2001;147:1765–74.
31. Liu J, Xu JZ, Rao ZM, Zhang WG. An enzymatic colorimetric whole-cell biosensor for high-throughput identification of lysine overproducers. Biosens Bioelectron. 2022;216:114681.
32. Wang Y, Li QG, Zheng P, Guo YM, Wang LX, Zhang TC, Sun JB, Ma YH. Evolving the L-lysine high-producing strain of *Escherichia coli* using a newly developed high-throughput screening method. J Ind Microbiol Biotech. 2016;43:1227–35.
33. Yang J, Seo SW, Jang S, Shin SI, Lim CH, Roh TY, Jung GY. Synthetic RNA devices to expedite the evolution of metabolite-producing microbes. Nat Commun. 2013;4:1413.
34. Wang JM, Gao DF, Yu XL, Li W, Qi QS. Evolution of a chimeric aspartate kinase for L-lysine production using a synthetic RNA device. Appl Microbiol Biotechnol. 2015;99:8527–36.
35. Xu JZ, Han M, Ren XD, Zhang WG. Modification of aspartokinase III and dihydrodipicolinate synthetase increases the production of L-lysine in *Escherichia coli*. Biochem Eng J. 2016;114:82–9.
36. Haywood GW, Large PJ. The occurrence, subcellular-localization and partial-purification of diamine acetyltransferase in the yeast *Candida boidinii* grown on spermidine or putrescine as sole nitrogen source. Eur J Biochem. 1985;148:277–83.
37. Samsonova NN, Smirnov SV, Altman IB, Ptitsyn LR. Molecular cloning and characterization of *Escherichia coli* K12 *ygjG* gene. BMC Microbiol. 2003;3:1.
38. Kurihara S, Oda S, Tsuboi Y, Kim HG, Oshida M, Kumagai H, Suzuki H. γ-glutamylputrescine synthetase in the putrescine utilization pathway of *Escherichia coli* K-12. J Biol Chem. 2008;283:19981–90.
39. Shen XL, Wang J, Li CY, Yuan QP, Yan YJ. Dynamic gene expression engineering as a tool in pathway engineering. Curr Opin Biotechnol. 2019;59:122–9.
40. Rouches MV, Xu Y, Cortes LBG, Lambert G. A plasmid system with tunable copy number. Nat Commun. 2022;13:3908.

Publisher's Note